

**François Hug, Nicolas A. Turpin, Arnaud Guével and Sylvain Dorel**

*J Appl Physiol* 108:1727-1736, 2010. First published Mar 18, 2010;

doi:10.1152/jappphysiol.01305.2009

**You might find this additional information useful...**

---

This article cites 36 articles, 19 of which you can access free at:

<http://jap.physiology.org/cgi/content/full/108/6/1727#BIBL>

Updated information and services including high-resolution figures, can be found at:

<http://jap.physiology.org/cgi/content/full/108/6/1727>

Additional material and information about *Journal of Applied Physiology* can be found at:

<http://www.the-aps.org/publications/jappl>

---

This information is current as of June 2, 2010 .

## Is interindividual variability of EMG patterns in trained cyclists related to different muscle synergies?

François Hug,<sup>1</sup> Nicolas A. Turpin,<sup>1</sup> Arnaud Guével,<sup>1</sup> and Sylvain Dorel<sup>2</sup>

<sup>1</sup>Laboratory “Motricité, Interactions, Performance” (EA 4334), University of Nantes, Nantes, France; <sup>2</sup>Research Department, Laboratory of Biomechanics and Physiology, National Institute for Sports, Paris, France

Submitted 19 November 2009; accepted in final form 17 March 2010

**Hug F, Turpin NA, Guével A, Dorel S.** Is interindividual variability of EMG patterns in trained cyclists related to different muscle synergies?. *J Appl Physiol* 108: 1727–1736, 2010. First published March 18, 2010; doi:10.1152/jappphysiol.01305.2009.—Our aim was to determine whether muscle synergies are similar across trained cyclists (and thus whether the same locomotor strategies for pedaling are used), despite interindividual variability of individual EMG patterns. Nine trained cyclists were tested during a constant-load pedaling exercise performed at 80% of maximal power. Surface EMG signals were measured in 10 lower limb muscles. A decomposition algorithm (nonnegative matrix factorization) was applied to a set of 40 consecutive pedaling cycles to differentiate muscle synergies. We selected the least number of synergies that provided 90% of the variance accounted for VAF. Using this criterion, three synergies were identified for all of the subjects, accounting for  $93.5 \pm 2.0\%$  of total VAF, with VAF for individual muscles ranging from  $89.9 \pm 8.2\%$  to  $96.6 \pm 1.3\%$ . Each of these synergies was quite similar across all subjects, with a high mean correlation coefficient for synergy activation coefficients ( $0.927 \pm 0.070$ ,  $0.930 \pm 0.052$ , and  $0.877 \pm 0.110$  for synergies 1–3, respectively) and muscle synergy vectors ( $0.873 \pm 0.120$ ,  $0.948 \pm 0.274$ , and  $0.885 \pm 0.129$  for synergies 1–3, respectively). Despite a large consistency across subjects in the weighting of several monoarticular muscles into muscle synergy vectors, we found larger interindividual variability for another monoarticular muscle (soleus) and for biarticular muscles (rectus femoris, gastrocnemius lateralis, biceps femoris, and semimembranosus). This study demonstrated that pedaling is accomplished by the combination of the similar three muscle synergies among trained cyclists. The interindividual variability of EMG patterns observed during pedaling does not represent differences in the locomotor strategy for pedaling.

nonnegative matrix factorization; redundancy; pedaling; electromyographic pattern

IT IS WELL DOCUMENTED THAT the motor system is highly redundant. As a consequence, a single motor task can be performed in many ways with a similar end result (1). This motor redundancy suggests that the nervous system is capable of producing different muscle activity patterns for a given movement. In this line, interindividual variability of electromyographic (EMG) activity recorded in 10 lower limb muscles during pedaling within a population of trained cyclists has been demonstrated (13, 15). More precisely, Hug et al. (15) showed a high interindividual variability of EMG patterns for biarticular muscles as a whole (e.g., gastrocnemius lateralis and rectus femoris) and for one monoarticular muscle (tibialis anterior). When these 10 muscle activity patterns are evaluated

individually, the functional implications of the various muscle patterns are difficult to interpret.

Recently, a technique has emerged that is capable of describing multiple patterns of muscle activity in an integrative fashion. EMG patterns recorded from numerous muscles have been decomposed into the summed activation of just a few muscle synergies (34, 35). These can be defined as low-dimensional modules formed by muscles activated in synchrony (i.e., with the similar specific time-varying profiles) (9, 17, 31–33). The decomposition algorithm used to identify muscle synergies has two components (Fig. 1): a fixed component (named “muscle synergy vectors” in this study), which represents the relative weighting of each muscle within each synergy, and a time-varying component (named “synergy activation coefficient” in this study), which represents the relative contribution of the muscle synergy to the overall muscle activity pattern (33).

A muscle synergy provides an attractive simplifying strategy for the control of complex movements because it reduces the number of output patterns that the nervous system must specify for a large number of muscles (27). For example, it has been demonstrated that five muscle synergies account for the majority of the variability in the surface EMG signals of 32 muscles during walking (19). Additionally, these synergies are associated with the major kinematic and kinetic events of the gait cycle (19). Results from Cheung et al. (6) suggest that most of the synergies used for generating locomotor behaviors are centrally organized, but their activations may be modulated by sensory feedback so that the final motor outputs can be adapted to the external environment.

With these elements in mind, a question arises: is the pedaling task produced by a combination of similar muscle synergies (i.e., the same number of synergies, the same synergy activation coefficients, and the same muscle synergy vectors) among a population of trained cyclists? Or does the interindividual variability of EMG patterns observed during pedaling imply the use of different locomotor strategies for pedaling? In fact, one would expect that the interindividual variability of the initial EMG patterns would lead to similar muscle synergies (with some interindividual variability) or to different muscle synergies (and thus to different locomotor strategies for pedaling).

Thus the purpose of the present study was to determine whether muscle synergies are similar across trained cyclists (and thus whether they use the same locomotor strategies for pedaling), despite interindividual variability of individual EMG patterns (13, 15). It is critical to address the question to better understand the differences in pedaling effectiveness (i.e., ability to efficiently orientate the total force on the pedal) (15, 22) or the pedaling mechanical efficiency (i.e., ability to

Address for reprint requests and other correspondence: F. Hug, Univ. of Nantes, Laboratory “Motricité, Interactions, Performance” (EA 4334), 25 bis boulevard Guy Mollet, BP 72206, 44322 Nantes cedex 3, France (e-mail: francois.hug@univ-nantes.fr).

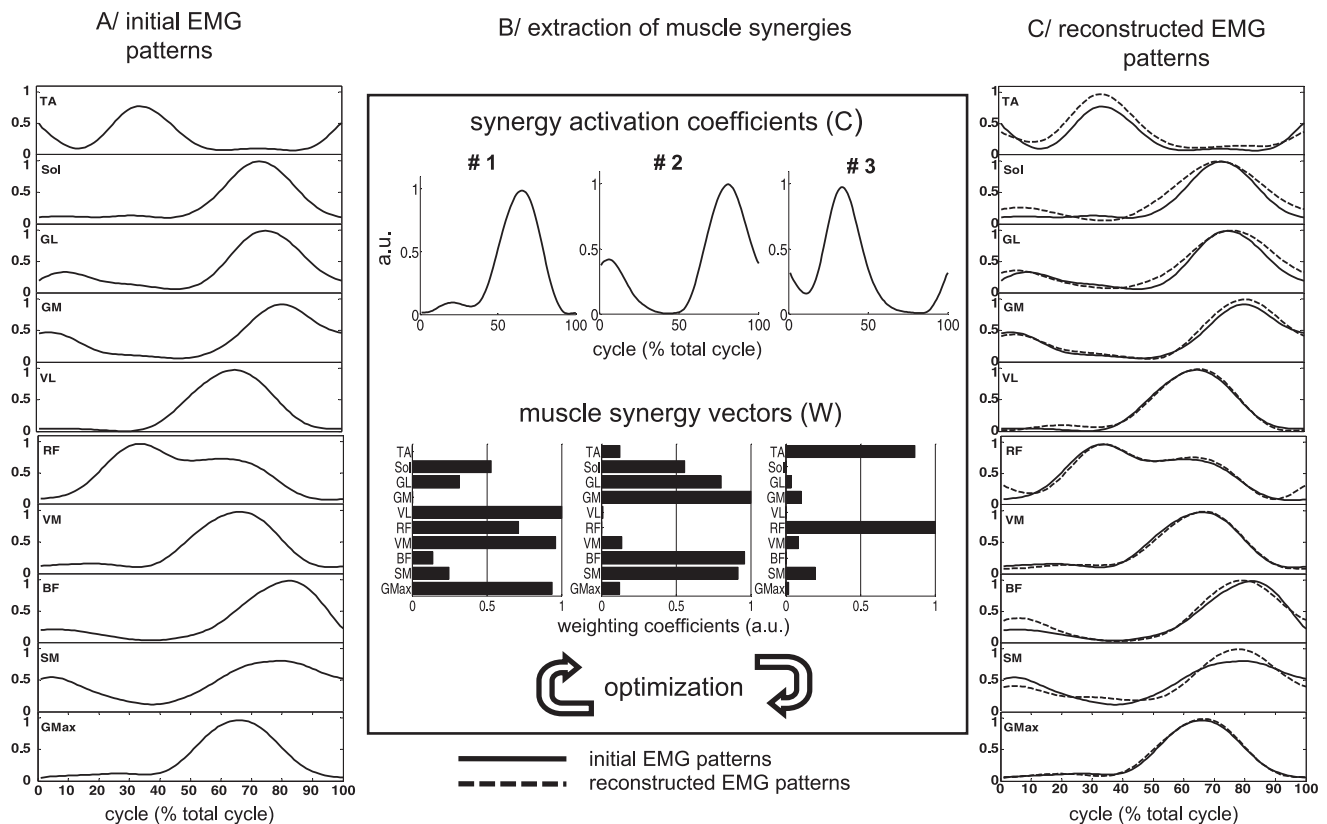


Fig. 1. Individual example of the extraction of muscle synergies. *A*: initial EMG patterns from 10 lower limb muscles (for clarity, only 1 pedaling cycle is depicted). *B*: EMG patterns were processed by a nonnegative matrix factorization algorithm, which applied an iterative optimization procedure to best reconstruct the initial EMG patterns using a small set of muscle synergies. For each muscle synergy, the adjusted parameters include the muscle synergy vectors (i.e., the relative weighting of each muscle within each synergy) and the synergy activation coefficients (i.e., the relative contribution of the muscle synergy to the overall muscle activity pattern). The contribution of any muscle synergy to a muscle EMG pattern is the product of the muscle weighting for this synergy times the synergy activation coefficient. au, Arbitrary units. *C*: for each muscle, the EMG pattern is reconstructed by adding the contribution of each muscle synergy. BF, biceps femoris; GL, gastrocnemius lateralis; GM, gastrocnemius medialis; GMax, gluteus maximus; RF, rectus femoris; SM, semimembranosus; SOL, soleus; TA, tibialis anterior; VL, vastus lateralis; VM, vastus medialis.

increase the ratio of mechanical power output on the metabolic energy input (22) in a homogenous population of cyclists. We hypothesize that 1) trained cyclists would exhibit the same number and similar muscle synergies, suggesting the use of similar locomotor strategies for pedaling, and 2) the relative weighting of some muscles within each muscle synergy vector would exhibit higher interindividual variability, which could be linked to the interindividual variability of some EMG patterns reported in the literature. To test these hypotheses, we utilized a nonnegative matrix factorization algorithm to identify muscle synergies during pedaling in a population of trained cyclists.

## METHODS

**Subjects.** Nine male experienced cyclists (age:  $21.9 \pm 5.2$  years; body mass:  $69.5 \pm 6.0$  kg; height:  $180 \pm 6$  cm; maximal power:  $387 \pm 24$  W, and maximal oxygen consumption:  $64.9 \pm 8.2$  ml  $\cdot$  min $^{-1}$   $\cdot$  kg $^{-1}$ ) volunteered to participate in this study. Eight of these nine subjects were already involved in a previous study that characterized interindividual variability of EMG patterns during pedaling (15). The subjects had  $8.6 \pm 3.2$  years of competitive cycling experience. In the season before experimentation, they had covered an average of  $13,222 \pm 4,430$  km. Before the volunteers gave their written consent to participate, they were informed of the possible risk and discomfort associated with the experimental procedures. The experimental design of the study was approved

by the Ethical Committee of Saint-Germain-en-Laye (acceptance no. 06016) and was carried out in accordance with the Declaration of Helsinki.

**Exercise protocol.** After a standardized warm-up, subjects were asked to perform a cycling exercise at a constant power output equal to 80% of the maximal power reached during a classical incremental exercise (corresponding to a mean power output of  $327 \pm 28$  W) for as long as possible. Subjects were asked to keep a constant pedaling rate, which was freely chosen at the end of the warm-up session. For the purpose of this study, only the second minute was taken into consideration for subsequent analysis of muscle synergies. The time to exhaustion for this pedaling protocol was  $\sim 14$  min; thus including only the second minute of the task reduces the chance of fatigue influencing EMG patterns and/or muscle synergies. This is supported by the results of Dorel et al. (11), which showed no EMG modification during the first 2 min of an identical pedaling exercise.

**Material and data collection.** Subjects exercised on an electronically braked cycle ergometer (Excalibur Sport, Lode, Groningen, The Netherlands) equipped with standard cranks (length = 170 mm). Vertical and horizontal positions of the saddle, handlebar height, and stem length were set to match the usual racing position of the participants (i.e., dropped posture).

Surface EMG activity was continuously recorded for the following 10 muscles in the right lower limb: gluteus maximus, semimembranosus, long head of biceps femoris, vastus medialis, rectus femoris, vastus lateralis, gastrocnemius medialis and lateralis, soleus, and

tibialis anterior. A pair of surface Ag/AgCl electrodes (Blue sensor, Ambu, Ballerup, Denmark) was attached to the skin with a 2-cm interelectrode distance. The electrodes were placed longitudinally with respect to the underlying muscle fiber arrangement and were located according to the recommendations of SENIAM (Surface EMG for Non-Invasive Assessment of Muscles) (12). Before the electrodes were applied, the skin was shaved and cleaned with alcohol to minimize impedance. The wires connected to the electrodes were well secured with adhesive tape to avoid movement-induced artifacts. A transistor-transistor logic pulse was used to detect the bottom dead center (BDC; lowest position of the right pedal with crank arm angle at 180°) of the right pedal. Raw EMG signals were amplified close to the electrodes (gain of 305 and bandwidth of 8–500 Hz) and simultaneously digitized with BDC transistor-transistor logic pulses at a sampling rate of 1 kHz (ME6000P16, Mega Electronics, Kuopio, Finland).

**Muscle synergy extraction.** EMG signals were high-pass filtered (20 Hz, Butterworth filter), rectified, and low-pass filtered (5 Hz, zero lag). Nonnegative matrix factorization was performed from a set of consecutive pedaling cycles as previously done by Clark et al. (8). The advantage of this is that cycle-to-cycle variability is taken into

account. This variability contains structured information that is important to establish robust synergy extraction. Factor analysis, independent component analysis, and nonnegative matrix factorization have all been previously utilized to extract muscle synergies from EMG signals. Although each of these statistical approaches places different restrictions on the outcomes, they all converge on a similar solution related to the temporal structure of the EMG activity pattern (34). As done in previous works (7, 16, 32), nonnegative matrix factorization was used in the present study. For this purpose, we implemented the Lee and Seung algorithm (23). Matrix factorization minimizes the residual Frobenius norm between the initial matrix and its decomposition, given as:

$$\mathbf{E} = \mathbf{WC} + \mathbf{e}$$

$$\begin{aligned} \min & \|\mathbf{E} - \mathbf{WC}\|_{\text{FRO}} \\ & \mathbf{W} \geq 0 \\ & \mathbf{C} \geq 0 \end{aligned}$$

where  $\mathbf{E}$  is a  $p$ -by- $n$  initial matrix ( $p$  is number of muscles and  $n$  is number of time points),  $\mathbf{W}$  is a  $p$ -by- $s$  matrix ( $s$  is number of synergies),  $\mathbf{C}$  is an  $s$ -by- $n$  matrix, and  $\mathbf{e}$  is a  $p$ -by- $n$  matrix in Eq. 1. In

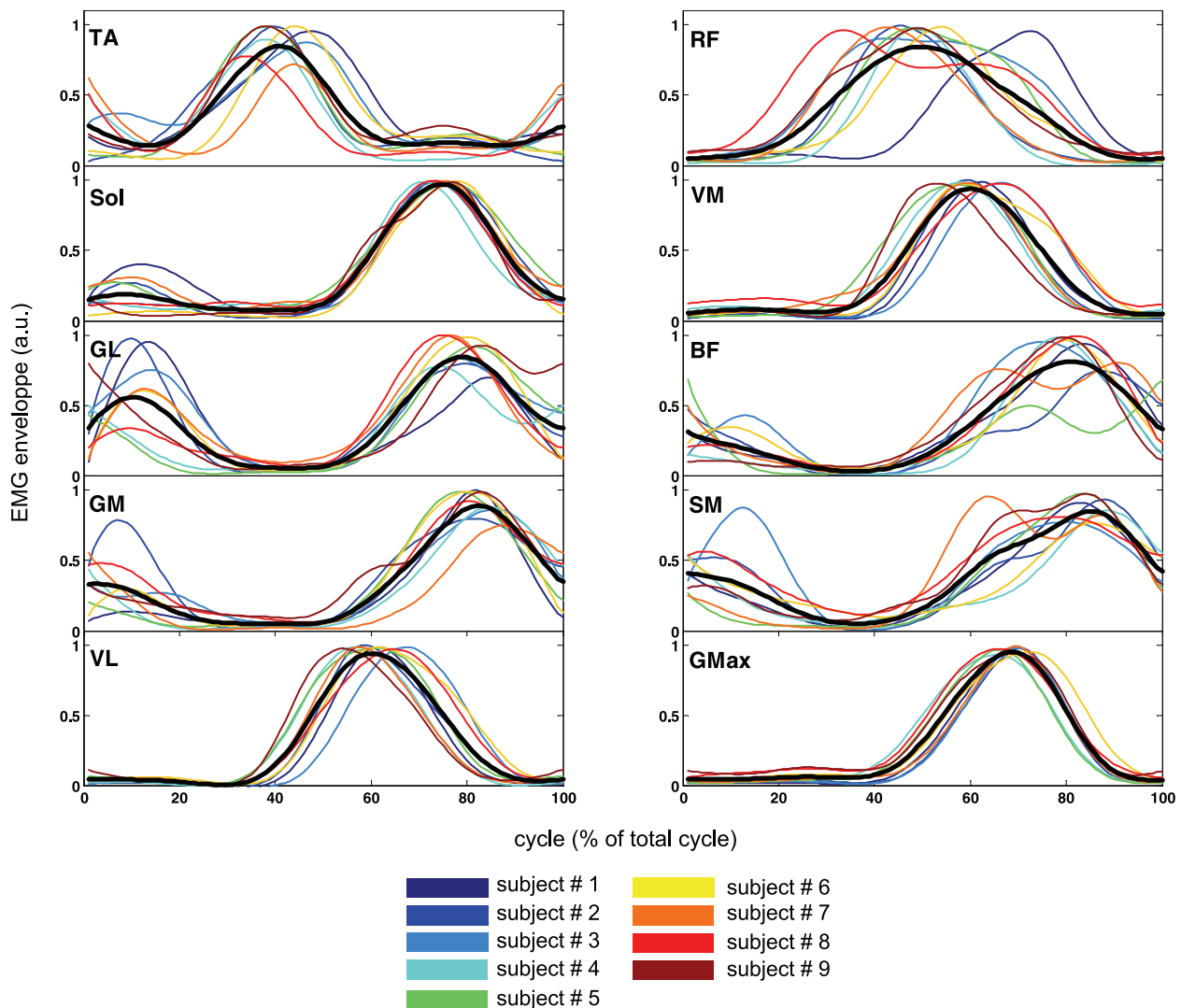


Fig. 2. EMG envelope for 10 lower limb muscles obtained in 9 subjects during pedaling. Each profile represents an individual EMG pattern averaged across 40 consecutive pedaling cycles and is expressed as a function of the percentage of the pedaling cycle as it rotated from the lowest pedal position [bottom dead center (BDC), 0%] to the highest [top dead center (TDC), 50%] and back to BDC to complete a 360° crank cycle. The bold black line indicates the mean profile across the 9 subjects. Each individual muscle pattern is normalized by the average of its peak from all cycles.

Table 1. Interindividual variability of the initial EMG patterns

Muscle	$r$	VR
Tibialis anterior	0.747 ± 0.155	0.269
Soleus	0.957 ± 0.026	0.058
Gastrocnemius lateralis	0.746 ± 0.164	0.275
Gastrocnemius medialis	0.884 ± 0.083	0.148
Vastus lateralis	0.909 ± 0.089	0.100
Rectus femoris	0.724 ± 0.296	0.315
Vastus medialis	0.889 ± 0.097	0.122
Biceps femoris	0.824 ± 0.120	0.206
Semimembranosus	0.810 ± 0.136	0.234
Gluteus maximus	0.963 ± 0.320	0.050

Values are means ± SD.  $r$ , Correlation coefficient; VR, variance ratio.

Eq. 2,  $\|\bullet\|_{FRO}$  establishes the Frobenius norm,  $\mathbf{W}$  represents the muscle synergy vectors matrix,  $\mathbf{C}$  is the synergy activation coefficients matrix, and  $\mathbf{e}$  is the residual error matrix. The algorithm is based on iterative updates of an initial random guess of  $\mathbf{W}$  and  $\mathbf{C}$  that converge to a local optimal matrix factorization [see Lee and Seung (23) for more details]. To avoid local minima, the algorithm was repeated 10 times for each subject. The lowest cost solution was kept (i.e., minimized squared error between original and reconstructed EMG patterns).

A pedaling cycle was defined as a complete revolution of the right pedal as it rotated from the lowest pedal position (0%, BDC) to the highest [50%, top dead center (TDC)] and back to BDC to complete a 360° crank cycle. The initial matrix  $\mathbf{E}$  consisted of 40 consecutive cycles for the 10 muscles. Each cycle was interpolated to 100 time points.  $\mathbf{E}$  was thus a 10-row and 4,000-column matrix. Each line of  $\mathbf{E}$  and  $\mathbf{C}$  was normalized by the average of its peak from all cycles. The muscle synergy vectors have been normalized by their maximum under the synergy to which they belong (24).

In all of our subjects, we iterated the analysis by varying the number of synergies between 1 and 10 and then selected the least number of synergies that accounted for >90% of variance accounted for (VAF) (32). To ensure that additional functional synergies did not exist, we compared all other synergies with each of the previously determined synergies. All additional synergies were similar in time varying profiles ( $r > 0.75$ ) to those previously determined. Thus, they were not retained.

**Variance calculation.** Mean total VAF was defined as (32):

$$\text{VAF} = 1 - \frac{\sum_{i=1}^p \sum_{j=1}^n (\mathbf{e}_{i,j})^2}{\sum_{i=1}^p \sum_{j=1}^n (\mathbf{E}_{i,j})^2}$$

VAF was also calculated for each muscle according to Torres-Oviedo and Ting (33), where VAF is defined as the uncentered Pearson correlation coefficient. Each vector of muscle activation was compared with its reconstruction as:

$$\text{VAF}_{\text{muscle}_m} = 1 - \frac{\sum_{i=1}^n (\mathbf{e}_{m,i})^2}{\sum_{i=1}^n (\mathbf{E}_{m,i})^2}$$

where subscript  $i$  goes from 1 to  $n$  (the number of time points),  $m$  represents the muscle  $m$  ( $m$  assumes a value of 1 to  $p$ , where  $p$  is the number of muscles).

**Assessment of interindividual variability.** To quantify the interindividual variability of the EMG patterns for each of the 10 recorded muscles, synergy activation coefficients ( $\mathbf{C}$ ) and muscle synergy vectors ( $\mathbf{W}$ ), we calculated the variance ratio (VR) and the Pearson correlation coefficient ( $r$ ). VR was determined according to the following equation (3):

$$\text{VR} = \frac{\sum_{i=1}^k \sum_{j=1}^s (X_{ij} - \bar{X}_i)^2 / k(s-1)}{\sum_{i=1}^k \sum_{j=1}^s (X_{ij} - \bar{X})^2 / (ks-1)} \quad \text{with} \quad \bar{X} = \frac{1}{k} \sum_{i=1}^k \bar{X}_i$$

where  $k$  is the number of measures (i.e., 100 for both EMG patterns and synergy activation coefficients and 10 for muscles synergies),  $s$  is the number of subjects (i.e., 9),  $\bar{X}$  is the mean values obtained at the  $i$ th interval calculated over the nine subjects, and  $X_{ij}$  is the value at the  $i$ th interval for the  $j$ th participant. Because it takes into account the amplitude of the curves, VR has been recently reported as an interesting index for assessing intrasubject and intersubject variability (3, 28). VR is directly related to the interindividual variability; therefore, a lower VR value reflects lower interindividual variability.

The  $r$  value was calculated by taking the averaged correlation coefficient between each pair of individual EMG patterns, between each pair of synergy activation coefficients (for each muscle synergy), and between each pair of muscle synergy vectors (for each muscle synergy). The correlation coefficient value has been used to assess similarity of muscle synergies in previous works (e.g., Refs. 16, 32).

## RESULTS

**Pedaling rate.** The pedaling exercise was achieved at a mean pedaling rate of  $93.9 \pm 5.5$  rpm (ranging from 87.2 to 104.6 rpm), corresponding to a relatively low coefficient of variation of 5.8%.

**Interindividual variability of the individual EMG patterns.** Individual EMG patterns for the 10 muscles investigated are depicted in Fig. 2. High intersubject variability is evident, particularly for some biarticular muscles (e.g., gastrocnemius lateralis, rectus femoris, semimembranosus, and biceps femoris) and one monoarticular muscle (tibialis anterior). Overall, this result is confirmed by the lowest  $r$  and highest VR for these five muscles (Table 1). In contrast, low interindividual variability was found for the four monoarticular muscles (gluteus maximus, soleus, vastus lateralis, and vastus medialis) for which lower VR and higher  $r$  values were observed.

**Muscle synergies extraction.** The cumulative percentage of variance explained by each synergy is shown in Fig. 3. Using the criteria previously described, we identified three synergies

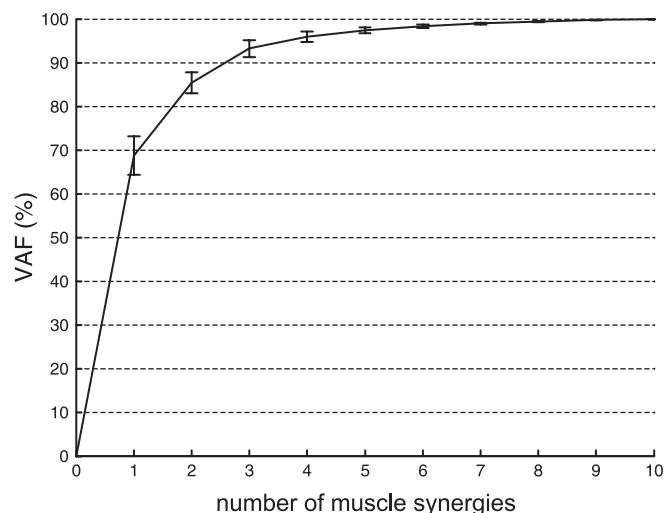


Fig. 3. Mean percentage of variance accounted for (VAF) as a function of the number of extracted synergies. Three synergies were identified for all the subjects, which accounted for  $93.5 \pm 2.0\%$  of total VAF.

Table 2. VAF depicted for each muscle for 3 extracted muscle synergies

Muscle	VAF
Tibialis anterior	94.8 ± 5.0
Soleus	92.5 ± 2.4
Gastrocnemius lateralis	90.1 ± 6.1
Gastrocnemius medialis	92.7 ± 4.5
Vastus lateralis	96.5 ± 2.0
Rectus femoris	94.8 ± 4.3
Vastus medialis	96.6 ± 1.3
Biceps femoris	89.9 ± 8.2
Semimembranosus	92.5 ± 4.0
Gluteus maximus	92.2 ± 3.3

Values are means ± SD. VAF, variance accounted for.

for all of the subjects, accounting for  $93.5 \pm 2.0\%$  of the total VAF (Fig. 3) and leading to VAF for individual muscles ranging from  $89.9 \pm 8.2\%$  (biceps femoris) to  $96.6 \pm 1.3\%$  (vastus medialis) (Table 2). Thus, three muscle synergies can reproduce initial EMG patterns for all subjects. An individual example of the synergy activation coefficients from 40 consecutive pedaling cycles is depicted in Fig. 4. The consistency of synergy activation coefficients across cycles was high (mean  $r$  calculated across the 40 consecutive cycles =  $0.996 \pm 0.09$ ,  $0.987 \pm 0.006$ , and  $0.980 \pm 0.016$  for synergies 1, 2, and 3, respectively). Figure 5 depicts muscle synergy vectors and synergy activation coefficients for all of the subjects. Each of the three independent synergies was quite similar across all subjects, with a high mean coefficient of correlation for both synergy activation coefficients ( $0.927 \pm 0.070$ ,  $0.930 \pm 0.052$ , and  $0.877 \pm 0.110$  for synergies 1, 2, and 3, respectively) and muscle synergy vectors ( $0.873 \pm 0.120$ ,  $0.948 \pm 0.274$ , and  $0.885 \pm 0.129$  for synergies 1, 2, and 3, respectively). For synergy activation coefficients, the VR was 0.080, 0.090, and

0.130 for synergies 1, 2, and 3, respectively. For muscle synergy vectors, VR was 0.150, 0.060, and 0.120 for synergies 1, 2, and 3, respectively.

The relative contribution of each muscle synergy to the overall muscle activity pattern was specified by the synergy activation coefficients (Fig. 5A). By analyzing both the synergy activation coefficients and the muscle synergy vectors, the following properties were identified for each muscle synergy. 1) *Synergy 1* mainly consists of extensor activity from the gluteus maximus, soleus, and three muscles of the quadriceps group (vastus lateralis, vastus medialis, and rectus femoris) (Fig. 5B). It is active during the downstroke phase of the pedaling cycle (Figs. 5A and 6B), with peak activity occurring during the first part of this phase. 2) *Synergy 2* is primarily active during the second part of the downstroke phase and, to a lesser extent, during the beginning of the upstroke phase (Figs. 5A and 6B). It consists of activity in the hamstrings group (semimembranosus and biceps femoris) and the plantar flexors (soleus, gastrocnemius medialis, and gastrocnemius lateralis) (Fig. 5B). 3) *Synergy 3* is active from the middle of the upstroke phase to the beginning of the downstroke phase (Figs. 5A and 6B). It mainly consists of the activity in the rectus femoris and tibialis anterior muscles (Fig. 5B).

*Intersubject variability of individual muscles within each muscle synergy vector.* The intersubject variability in the weighting of each muscle within the muscle synergy vectors is depicted in Fig. 7. Despite consistency across subjects for several monoarticular muscles (e.g., vastus lateralis, vastus medialis, gluteus maximus), there was greater intersubject variability in one monoarticular muscle (soleus in synergy 2) and in biarticular muscles (e.g., rectus femoris in synergies 1 and 3, gastrocnemius lateralis in synergy 1, biceps femoris in synergies 1 and 2, and semimembranosus in synergy 1).

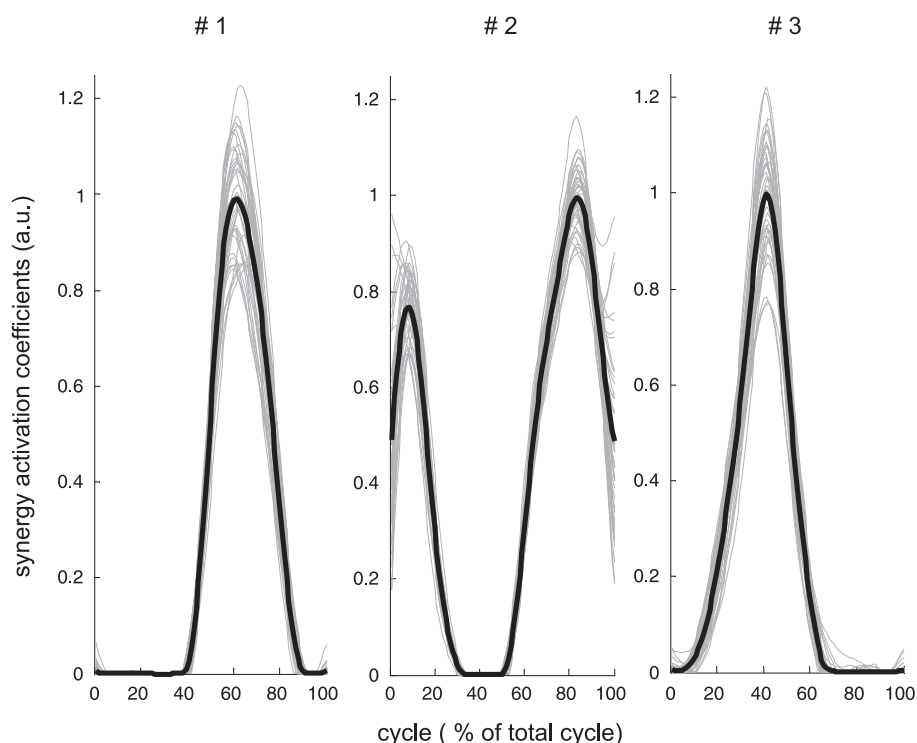


Fig. 4. Individual example of the 3 extracted synergy activation coefficients. Three synergy activation coefficients were extracted from a set of 40 consecutive pedaling cycles. Bold lines represent means of 40 cycles. The synergy activation coefficients are expressed as a function of the percentage of the pedaling cycle as it rotated from the lowest pedal position (BDC, 0%) to the highest (TDC, 50%) and back to BDC to complete a 360° crank cycle. Cycle-to-cycle variability is accounted for by this technique. This example demonstrates that the activation of the 3 muscle synergies is very consistent across the 40 consecutive cycles (gray lines).

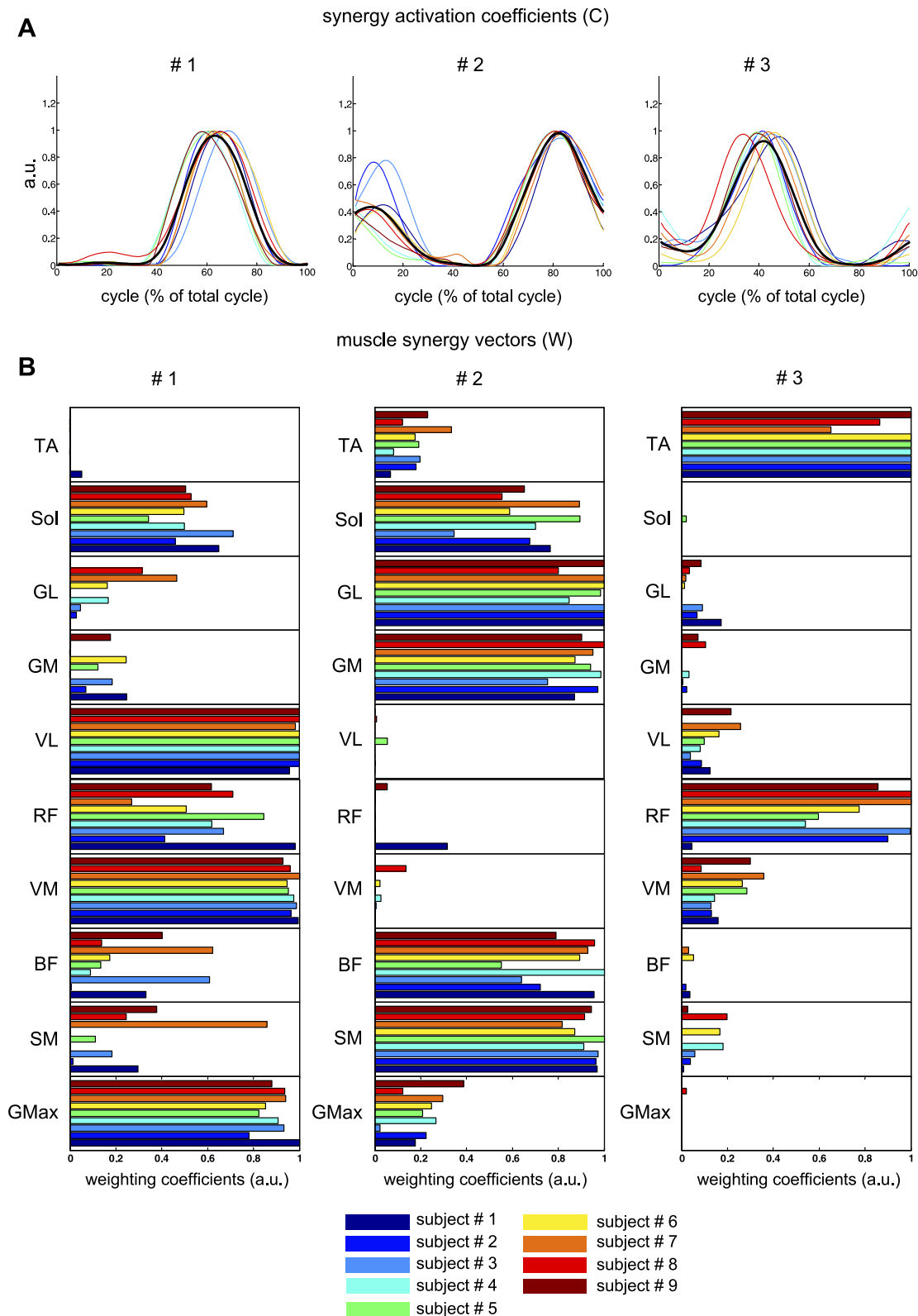


Fig. 5. Synergy activation coefficients (C) and muscle synergy vectors (W) across the 9 subjects. A: synergy activation coefficients for all the subjects and for the 3 extracted synergies (solid lines in different colors). The synergy activation coefficients are expressed as a function of the percentage of the crank arm cycle as it rotated from the lowest pedal position (BDC, 0%) to the highest (TDC, 50%) and back to BDC to complete a 360° crank cycle. Between-subject comparisons have been made possible by normalizing each muscle by the average of its peak from all cycles. The mean synergy activation coefficient over all subjects is represented by the bold black line. B: muscle synergy vectors for all the subjects. Individual muscle weightings are depicted for each muscle within each synergy. The muscle synergy vectors have been normalized by their maximum under the synergy to which they belong.

A (adapted from Raasch and Zajac, 1999)

B

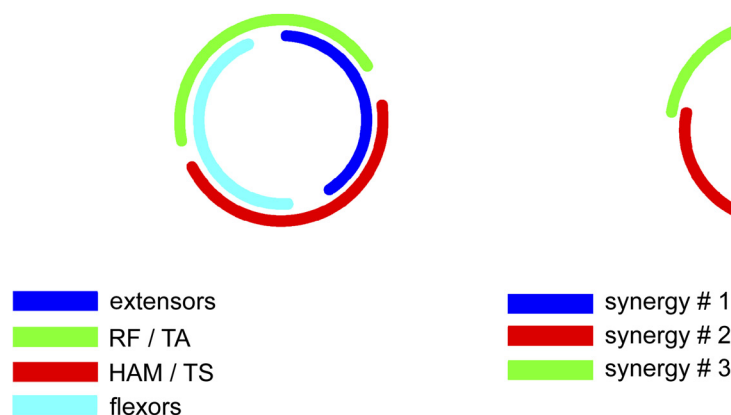


Fig. 6. A: schematic representation of the results reported by Raasch and Zajac (27). B: schematic representation of the 3 muscle synergies found in the present study. Numbers refer to the 4 functional sectors defined by Hug et al. (15). HAM, hamstrings; TS, ankle plantar flexors.

## DISCUSSION

This study used a nonnegative matrix factorization algorithm to identify muscle synergies in trained cyclists. The similar three muscle synergies were found across subjects despite distinct differences in the individual EMG patterns of some muscles. Despite a major consistency across subjects in the weighting of most monoarticular muscles into muscle synergy vectors, there was larger intersubject variability for the soleus, a monoarticular muscle, and for biarticular muscles (rectus femoris, gastrocnemius lateralis, biceps femoris, and semimembranosus).

*Functional significance of the extracted muscle synergies.* To our knowledge, only one study has extracted muscle synergies during pedaling (37). However, since the methodology used to extract muscle synergies was very different from that used in the present study (i.e., principal component analysis and especially a presupposed number of muscle synergies = 6), a direct comparison is very difficult to conduct and interpret. Based on simulation, Raasch and Zajac (27) proposed a simple control scheme of pedaling, consisting of a four muscle group control (Fig. 6A). The results of the present study were very similar to this model (27). *Synergy 1* mainly utilized three knee extensors (i.e., vastus lateralis, vastus medialis, rectus femoris) and one hip extensor (i.e., gluteus maximus) and thus corresponds to the first muscle group defined by Raasch and Zajac (27), which produces energy needed to propel the crank through limb extension. When we take into account an electromechanical delay, this synergy is highly related to the effective force profile reported by various previous studies (11). It is in line with previous observations made by Ivanenko et al. (17) showing that muscle synergies are associated with the major kinematic and kinetic events during gait. *Synergy 2* mainly comprised the hamstrings and ankle plantar flexors (Fig. 5B) and thus corresponds to the third muscle group of Raasch and Zajac (27), which produces energy to propel the crank during the second part of the downstroke phase and during the limb transition from extension to flexion. Finally, *synergy 3* mainly implied the tibialis anterior and the rectus femoris and thus corresponds to their fourth muscles group, which acts at the end of the limb flexion and during the limb transition from flexion to extension. The second muscle group (i.e., the monoarticular hip and knee flexor muscles) identified by Raasch and Zajac (27), which acted during the upstroke phase, was not represented by the extracted synergies in the

present study. This difference is likely due to the fact that we did not record EMG activity in monoarticular hip and knee flexors (e.g., psoas major, short head of the biceps femoris and popliteus). These muscles are more difficult to record using surface EMG. For instance, the psoas major is a deep muscle and not able to be assessed with surface EMG (21). Deeper muscles can only be recorded with intramuscular electrodes. However, intramuscular recordings, even when measured with wire electrodes, sample a limited number of motor units; thus the signal is not necessarily representative of the global muscle activity (2). Overall, although we have recorded the main surface muscles utilized in the pedaling task (14), additional deep muscles may have possibly led to more muscles belonging to each synergy or to additional extracted synergies.

Interestingly, *synergies 1* and *3* from the present work are very similar to some synergies (in terms of both muscle synergy vectors and synergy activation coefficients) extracted during human walking (25). *Synergy 1* would correspond to the muscle synergy composed principally by gluteus medius and vastii and rectus femoris (*module 1* from Ref. 25), contributing to body support in early stance. *Synergy 3* would correspond to the muscle synergy composed of the rectus femoris and tibialis anterior (*module 3* from Ref. 25), which acts to decelerate the leg in early and late swing while generating energy to the trunk throughout swing. This observation is consistent with previous results that showed that there are similarities among the synergies extracted from different behaviors in frogs (10). Thus it would represent further evidence that the central nervous system utilizes similar combining muscle synergies for the construction of different types of locomotion.

*Interindividual variability.* Few previous studies have focused on the heterogeneity of lower limb EMG patterns during pedaling (13, 15, 29). The interindividual variability of individual EMG patterns (i.e., each of the EMG patterns recorded in the 10 muscles) reported in the present study is very similar to the results reported by Hug et al. (15) at lower power outputs (i.e., 150 and 250 W). It is notable that highly different individual patterns for some biarticular muscles (e.g., rectus femoris, semimembranosus, and biceps femoris) were observed. The novelty of our present work is that we aimed to determine whether this interindividual variability is related to different muscle synergies across trained cyclists. The main result that we found was the same number of muscle synergies

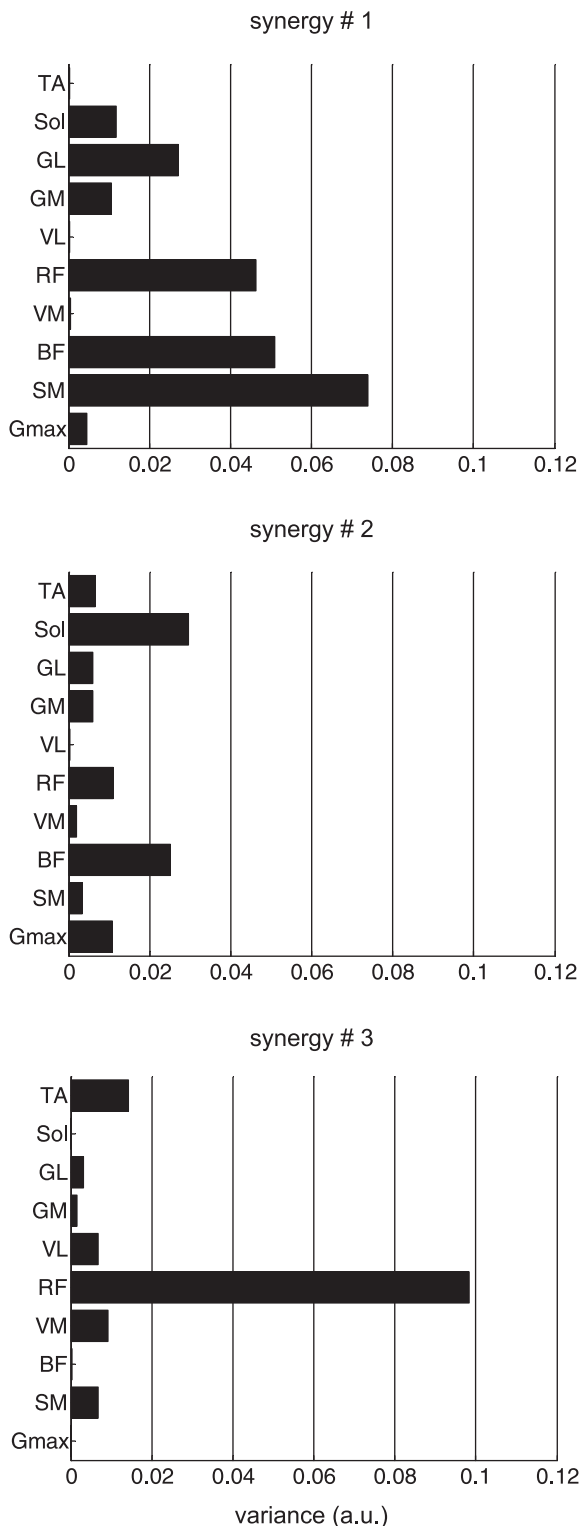


Fig. 7. Interindividual variance is depicted for each muscle within each muscle synergy vector. The variance is the squared standard deviation.

(i.e., three) accounting for the EMG activity patterns of 10 lower limb muscles during pedaling among trained cyclists. As performed in numerous other studies (4, 8, 16), we also assessed the similarity of each of these three synergies across subjects by calculating the coefficient of correlation. With

regard to the high  $r$  values found for both synergy activation coefficients (0.927, 0.930, and 0.877 for *synergies 1, 2, and 3*, respectively) and muscle synergy vectors (0.873, 0.948, and 0.885 for *synergies 1, 2, and 3*, respectively), we can reasonably conclude that the same three very similar functional muscle synergies are used by each of the trained cyclists (Fig. 5). Thus we can make the hypothesis that similar locomotor strategies for pedaling are used by each cyclist.

By performing a nonnegative matrix factorization, it could be hypothesized that the original variability is partially lost and thus that the three similar muscle synergies do not characterize the intersubject variability of the individual EMG patterns. However, the high mean VAF value ( $93.5 \pm 2.0\%$ ) and the high VAF values obtained for each muscle (Table 2; from  $89.9 \pm 8.2\%$  to  $96.6 \pm 1.3\%$ ) demonstrate that each EMG pattern, even for the most variable muscles, was well reconstructed by the three similar muscle synergies. For instance, Fig. 8 shows that the three similar muscle synergies (i.e.,  $r$  values ranged from 0.826 to 0.888 for synergy activation coefficients and  $r$  values ranged from 0.923 to 0.939 for muscle synergy vectors) have been extracted for three subjects who have very different initial EMG patterns for some muscles (e.g.,  $r = 0.726, 0.754, 0.770$ , and  $0.776$  for semimembranosus, tibialis anterior, gastrocnemius lateralis, and rectus femoris, respectively) and that these differences are already present in the reconstructed EMG patterns. Thus we can conclude that the similarity found is not due to the loss of intersubject variability by the nonnegative matrix factorization.

Despite this similarity, the individual muscle synergy vectors and synergy activation coefficients were in some cases more variable because there were definite individual differences. These differences should certainly explain a part of the interindividual variability of individual EMG patterns. For instance, Fig. 7 shows interindividual variability in the weighting of some muscles into muscle synergy vectors, particularly for biarticular muscles (rectus femoris, gastrocnemius lateralis, biceps femoris, semimembranosus). This is in accordance with previous observations (13, 15, 29) and is consistent with the fact that these muscles function to transfer energy between joints and control the direction of force production (36). To a lesser extent, an interindividual variability for soleus (monoarticular muscle) also exists that can be linked to its role of ankle stabilization during downstroke/upstroke transition (*synergy 2*). In contrast, the consistency of the weightings in several monoarticular muscles (e.g., vastus lateralis, vastus medialis, gluteus maximus) is akin to previous works that have reported the muscle activity pattern of monoarticular muscles to be less variable (13, 15, 29). This low variability is likely related to the fact that these monoarticular muscles act primarily in concentric mode as power producers during pedaling (36). Interestingly, the fact that higher interindividual variability was found for *synergy 3* is in accordance with the higher interindividual variability of mechanical effectiveness reported during the upstroke/downstroke transition (15).

**Methodological considerations.** EMG patterns of lower limb muscles during pedaling can be influenced by numerous factors, including body position and shoe-pedal interface (14). For this reason, all of these parameters were standardized in the present work. Since EMG activity can be altered by modulations in the pedaling rate, this was mainly observed for large changes [e.g., 45–120 rpm (26)]. For modest changes in the pedaling rate, as observed in our study, EMG activity level is

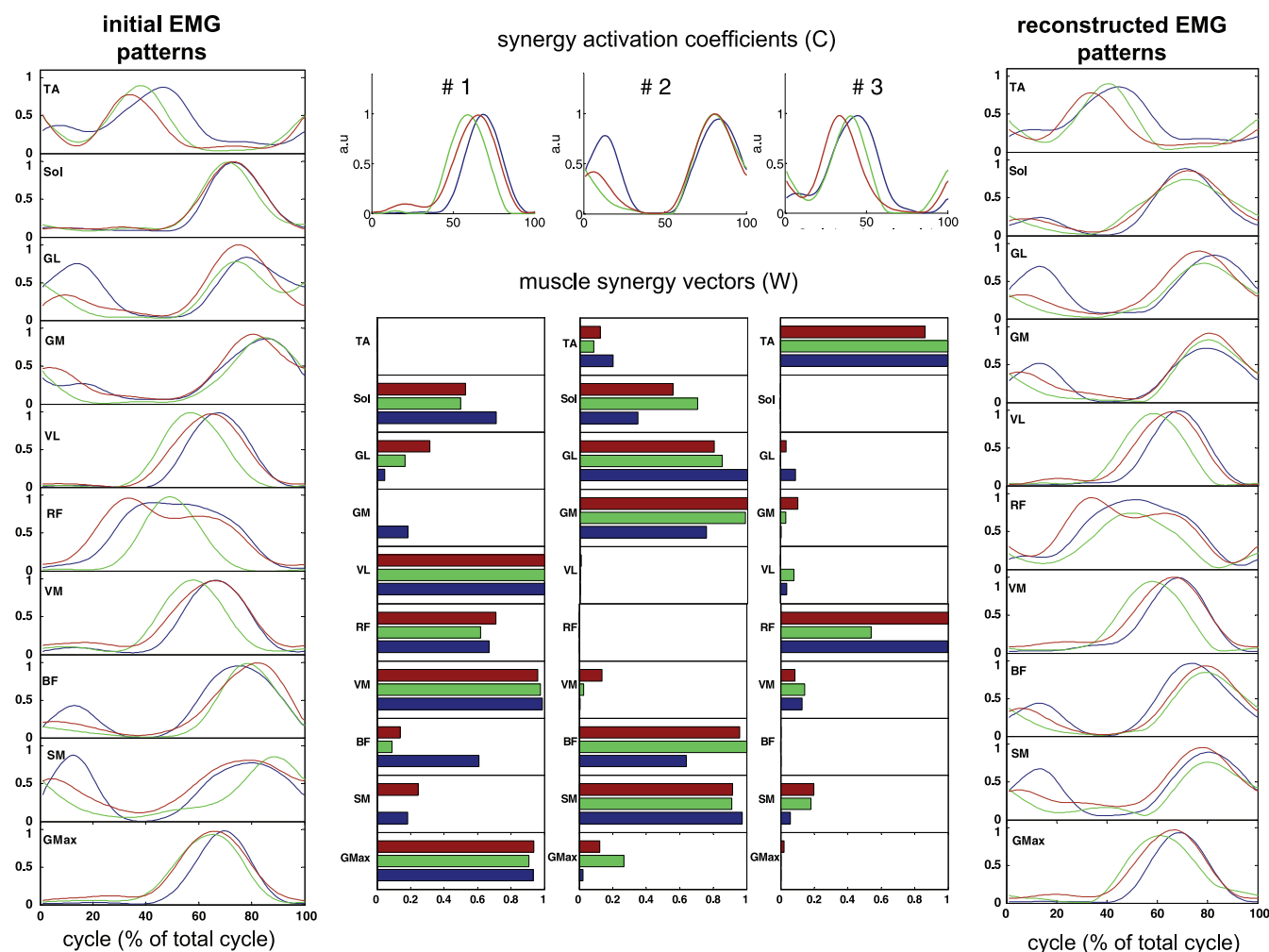


Fig. 8. Extraction of muscle synergies in cyclists ( $n = 3$ ) with different initial EMG patterns. Despite these different EMG patterns, 3 similar synergies were extracted. Interestingly, when EMG patterns are reconstructed using these synergies, the variability of the initial EMG patterns reappears, demonstrating that the variability is not lost by the nonnegative matrix factorization.

slightly modified and the time-varying profile does not vary (14). Thus it can be reasonably hypothesized that the low intersubject variability for pedaling rate did not influence our results.

A potential limitation of the present study is the possibility of cross talk between EMG channels. Because of the method of EMG analysis (i.e., nonnegative matrix factorization) that we used in this study, any cross talk might exaggerate a positive correlation. However, Chapman et al. (5) performed both surface and intramuscular EMG recordings in leg muscles during pedaling and reported that these two recordings produced similar activation patterns. In addition, as mentioned by Ivanenko et al. (18), cross talk would be limited to only a few of the 10 recorded muscles. Therefore, it is unlikely that the muscle synergies observed herein would be significantly biased. If cross talk did exist, it would most likely have primarily affected the muscle synergy vectors as suggested by Ivanenko et al. (18).

EMG activity from each muscle was normalized to the average of its peak value from all of the 40 cycles, similar to previous studies evaluating muscle synergies (30, 32). It should be noted that this normalization procedure only provides information about the level of muscle activity in relation to this peak value (i.e., shape of the EMG pattern). Thus the absolute

level of EMG activity is not taken into consideration, making it difficult to directly quantify the power output contributions from each muscle synergy. For instance, the upstroke phase of the pedaling cycle in submaximal conditions is known to result in a moderate negative effective force (11). Therefore, *synergy 3* may contribute much less to the overall power output than the two other muscle synergies.

Finally, the interindividual differences in the weighting of some muscles into muscle synergy vectors could be partly explained by the heterogeneity of activity level within each muscle (38) and potentially due to the relative placement of the recording electrodes. However, this methodological consideration could not explain the totality of interindividual variability in some muscles into muscle synergy vectors because the electrode placement was performed by the same investigator for each subject utilizing standardized placement criteria. In this way, a second experiment was performed in one subject (*subject 9*) with no landmark to replace the EMG electrodes. The results showed very little variability in muscle synergies between the two tests and thus suggested a good repeatability. For these reasons, it has been reasonably hypothesized that our findings were not associated with any electrode location variability among subjects.

In conclusion, the present work showed that the same number (i.e., three) and similar synergies were found across trained cyclists, despite the interindividual variability of the initial EMG patterns. Therefore, the interindividual variability of EMG patterns observed by previous studies (13, 15) does not represent differences in the overall locomotor strategy for pedaling; rather, it could represent differences in the contribution of some muscles into the muscle synergy vectors. Because both synergy activation coefficients and muscle synergy vectors have been shown to be modulated by skill learning (20), it would be interesting to compare trained cyclists and untrained subjects.

#### ACKNOWLEDGMENTS

The authors thank Dr. Antoine Nordez and Dr. Thibault Deschamps for helpful comments during the revision process.

#### GRANTS

This study was funded in part by the French Ministry of Sport (contract No. 06-046). N. A. Turpin was supported by a scholarship of the "Région Pays de la Loire" (Project OPERF2A).

#### DISCLOSURES

No conflicts of interest, financial or otherwise, are declared by the authors.

#### REFERENCES

- Bernstein N. Coordination and regulation of movements. New York: Pergamon, 1967.
- Brown SH, Brookham RL, Dickerson CR. High-pass filtering surface EMG in an attempt to better represent the signals detected at the intramuscular level. *Muscle Nerve* 41: 234–239, 2010.
- Burden AM, Trew M, Baltzopoulos V. Normalisation of gait EMGs: a re-examination. *J Electromyogr Kinesiol* 13: 519–532, 2003.
- Cappellini G, Ivanenko YP, Poppele RE, Lacquaniti F. Motor patterns in human walking and running. *J Neurophysiol* 95: 3426–3437, 2006.
- Chapman AR, Vincenzino B, Blanch P, Knox JJ, Hodges PW. Intramuscular fine-wire electromyography during cycling: repeatability, normalisation and a comparison to surface electromyography. *J Electromyogr Kinesiol* 20: 108–117, 2010.
- Cheung VC, d'Avella A, Tresch MC, Bizzi E. Central and sensory contributions to the activation and organization of muscle synergies during natural motor behaviors. *J Neurosci* 25: 6419–6434, 2005.
- Cheung VC, d'Avella A, Bizzi E. Adjustments of motor pattern for load compensation via modulated activations of muscle synergies during natural behaviors. *J Neurophysiol* 101: 1235–1257, 2009.
- Clark DJ, Ting LH, Zajac FE, Neptune RR, Kautz SA. Merging of healthy motor modules predicts reduced locomotor performance and muscle coordination complexity post-stroke. *J Neurophysiol* 103: 844–857, 2010.
- d'Avella A, Bizzi E. Shared and specific muscle synergies in natural motor behaviors. *Proc Natl Acad Sci USA* 102: 3076–3081, 2005.
- d'Avella A, Saltiel P, Bizzi E. Combinations of muscle synergies in the construction of a natural motor behavior. *Nat Neurosci* 6: 300–308, 2003.
- Dorel S, Drouet JM, Couturier A, Champoux Y, Hug F. Changes of pedaling technique and muscle coordination during and exhaustive exercise. *Med Sci Sports Exerc* 41: 1277–1286, 2009.
- Hermens HJ, Freriks B, Disselhorst-Klug C, Rau G. Development of recommendations for SEMG sensors and sensor placement procedures. *J Electromyogr Kinesiol* 10: 361–374, 2000.
- Hug F, Bendahan D, Le Fur Y, Cozzone PJ, Grelot L. Heterogeneity of muscle recruitment pattern during pedaling in professional road cyclists: a magnetic resonance imaging and electromyography study. *Eur J Appl Physiol* 92: 334–342, 2004.
- Hug F, Dorel S. Electromyographic analysis of pedaling: a review. *J Electromyogr Kinesiol* 19: 182–198, 2009.
- Hug F, Drouet JM, Champoux Y, Couturier A, Dorel S. Interindividual variability of electromyographic patterns and pedal force profiles in trained cyclists. *Eur J Appl Physiol* 104: 667–678, 2008.
- Ivanenko YP, Cappellini G, Dominici N, Poppele RE, Lacquaniti F. Coordination of locomotion with voluntary movements in humans. *J Neurosci* 25: 7238–7253, 2005.
- Ivanenko YP, Grasso R, Zago M, Molinari M, Scivoletto G, Castellano V, Macellari V, Lacquaniti F. Temporal components of the motor patterns expressed by the human spinal cord reflect foot kinematics. *J Neurophysiol* 90: 3555–3565, 2003.
- Ivanenko YP, Poppele RE, Lacquaniti F. Five basic muscle activation patterns account for muscle activity during human locomotion. *J Physiol* 556: 267–282, 2004.
- Ivanenko YP, Poppele RE, Lacquaniti F. Motor control programs and walking. *Neuroscientist* 12: 339–348, 2006.
- Kargo WJ, Nitz DA. Early skill learning is expressed through selection and tuning of cortically represented muscle synergies. *J Neurosci* 23: 11255–11269, 2003.
- Keagy RD, Brumlik J, Bergan JL. Direct electromyography of the psoas major muscle in man. *J Bone Joint Surg Am* 48: 1377–1382, 1966.
- Korff T, Romer LM, Mayhew I, Martin JC. Effect of pedaling technique on mechanical effectiveness and efficiency in cyclists. *Med Sci Sports Exerc* 39: 991–995, 2007.
- Lee DD, Seung HS. Algorithms for nonnegative matrix factorization. advances in neural information processing systems. In: *Advances in Neural Processing Systems. Proceedings of the 2000 Conference*. Cambridge, MA: MIT Press, 2001, p. 556–562.
- Muceli S, Boye AT, d'Avella A, Farina D. Identifying representative synergy matrixes for describing muscular activation patterns during multi-directional reaching in the horizontal plane. *J Neurophysiol* 103: 1532–1542, 2010.
- Neptune RR, Clark DJ, Kautz SA. Modular control of human walking: a simulation study. *J Biomech* 42: 1282–1287, 2009.
- Neptune RR, Kautz SA, Hull ML. The effect of pedaling rate on coordination in cycling. *J Biomech* 30: 1051–1058, 1997.
- Raasch CC, Zajac FE. Locomotor strategy for pedaling: muscle groups and biochemical functions. *J Neurophysiol* 82: 515–525, 1999.
- Rouffet DM, Hautier CA. EMG normalization to study muscle activation in cycling. *J Electromyogr Kinesiol* 18: 866–878, 2007.
- Ryan MM, Gregor RJ. EMG profiles of lower extremity muscles during cycling at constant workload and cadence. *J Electromyogr Kinesiol* 2: 69–80, 1992.
- Ting LH, Macpherson JM. A limited set of muscle synergies for force control during a postural task. *J Neurophysiol* 93: 609–613, 2005.
- Ting LH, McKay JL. Neuromechanics of muscle synergies for posture and movement. *Curr Opin Neurobiol* 17: 622–628, 2007.
- Torres-Oviedo G, Macpherson JM, Ting LH. Muscle synergy organization is robust across a variety of postural perturbations. *J Neurophysiol* 96: 1530–1546, 2006.
- Torres-Oviedo G, Ting LH. Muscle synergies characterizing human postural responses. *J Neurophysiol* 98: 2144–2156, 2007.
- Tresch MC, Cheung VC, d'Avella A. Matrix factorization algorithms for the identification of muscle synergies: evaluation on simulated and experimental data sets. *J Neurophysiol* 95: 2199–2212, 2006.
- Tresch MC, Saltiel P, Bizzi E. The construction of movement by the spinal cord. *Nat Neurosci* 2: 162–167, 1999.
- Van Ingen Schenau GJ, Boots PJ, de Groot G, Snackers RJ, van Woensel WW. The constrained control of force and position in multi-joint movements. *Neuroscience* 46: 197–207, 1992.
- Wakeling JM, Horn T. Neuromechanics of muscle synergies during cycling. *J Neurophysiol* 101: 843–854, 2009.
- Zijdwind I, Kernell D, Kukulka CG. Spatial differences in fatigue-associated electromyographic behaviour of the human first dorsal interosseus muscle. *J Physiol* 483: 499–509, 1995.